A Journal of the Gesellschaft Deutscher Chemiker
Angewandte Chemie
International Edition
GDCh
www.angewandte.org

Accepted Article

Title: Water can Crosslink a Single Poly(ionic liquid) into Porous Supramolecular Membranes

Authors: Hong Wang, Yue Shao, Yong-Lei Wang, Xiangshuai Li, Atefeh Khorsand Kheirabad, Qiang Zhao, and Jiayin Yuan

To be cited as: *Angew. Chem. Int. Ed.* 10.1002/anie.202002679

Link to VoR: https://doi.org/10.1002/anie.202002679

WILEY-VCH

COMMUNICATION

Water can Crosslink a Single Poly(ionic liquid) into Porous Supramolecular Membranes

Yue Shao[a‡], Yong-Lei Wang[b‡], Xiangshuai Li[a], Atefeh Khorsand Kheirabad[b], Qiang Zhao[c], Jiayin Yuan[b], Hong Wang[a*]

Abstract: Reversible regulation of membrane microstructures *via* non-covalent interactions is of considerable interest yet remains a challenge. Herein, we discover a general one-step approach to fabricate supramolecular porous polyelectrolyte membranes (SPPMs) from a single poly(ionic liquid) (PIL). The experimental results and theoretical simulation suggested that SPPMs were formed by a hydrogen bond-induced phase separation of a PIL between its polar and apolar domains, which were linked together by water molecules. This unique feature was capable of modulating microscopic porous architectures and thus the global mechanical property of SPPMs by a rational design of the molecular structure of PILs. Such SPPMs could switch porosity upon thermal stimuli, as exemplified by dynamically adaptive transparency to thermal fluctuation. This finding provides fascinating opportunities for creating multifunctional SPPMs.

Porous polyelectrolyte membranes (PPMs) are appealing materials in modern science, engineering and technology because of a synergy between their distinctive charged nature and pore-confinement effects for applications ranging from electronic devices, adsorption/separation technology, lubrication, bioengineering, battery and more [1-6]. Traditionally, PPMs or their hybrids were constructed by self-assembly of block copolymers and multicomponent polymeric materials driven by electrostatic interaction, plus covalent crosslinking if needed [7,8]. These methods including the preparation of precursors are synthetically demanding, and/or time-/labor intensive. As such, alternative approaches have been devoted to accessing freestanding PPMs. Poly(ionic liquid)s (PILs) recently emerge as non-conventional polyelectrolytes that contain an IL species in their repeating unit [9,10], providing a multifunctional materials platform in the membrane field [11,12]. Recently, we developed scalable freestanding PPMs by electrostatic crosslinking of a hydrophobic PIL with a PIL-derived polyanion[13]; this discovery spawned a myriad of functional materials for various applications[13,14]. However, challenges remain here to make PPMs structurally reversible and reusable to become adaptive smart materials.

Supramolecular polymeric materials, in which reversible noncovalent interactions (*i.e.* H-bonding, π-π and *van der waals* interaction) hold them together, have been popularly studied because of their smart responsiveness toward external stimuli as well as reversibility and reusability[15-17]. Supramolecular porous polyelectrolyte membranes (SPPMs) that combines the characteristics of supramolecular materials and PPMs, represent an emerging type of advanced materials. However, fabrication of SPPMs from conventional polyelectrolyte is a great challenge owing to their intrinsic water solubility and complex bonding mode.

Herein, we discovered that a unique group of SPPMs could be readily fabricated from a single PIL-based route *via* H-bonding. The microstructures, functionalities, and mechanical properties of SPPMs can be tailored by varying the structural motifs in the used PIL. Due to their noncovalent and dynamic nature, such SPPMs reversibly switched porosity, a behavior that is useful to design smart optical windows.

Scheme 1. (a) Chemical structures of four PILs studied in this work. (b) Schematic illustration of the preparation procedure of SPPMs. The photograph on the right is a representative paper-like SPPM in size of 14 cm x 16 cm.

Four PILs of different chemical structures, where **PIL1** to **PIL-3** are poly(1,2,4-triazolium)s and **PIL-4** is a polyimidazolium, have been synthesized and tested for the preparation of SPPMs (Scheme 1a). Detailed information of the PIL synthesis and structural characterizations is provided in the supporting information, Figure S1-S14. In a typical membrane fabrication procedure as shown in Scheme 1b, a PIL solution in N, N-dimethylformamide (DMF) or any other solvents was drop-cast onto a glass mold (14 cm x 16 cm), dried 3 hours at 80 °C into a smooth transparent yellowish film at room temperature. The film together with its underlying glass was annealed in water for 12 h to afford SPPMs. Here only water was involved to develop hydrogen bonds to build up pores, making this approach straightforward, eco-friendly, and scalable in size and quantity.

---

[a] Mr. Y. Shao, Mr. X. Li, Prof. H. Wang
Key Laboratory of Functional Polymer Materials of the Ministry of Education, Institute of Polymer Chemistry, College of Chemistry
Nankai University
Tianjin, 300071, P. R. China
E-mail: hongwang1104@nankai.edu.cn
[b] Dr. Y. L. Wang, Miss A. K. Kheirabad, Prof. J. Yuan
Department of Materials and Environmental Chemistry
Stockholm University
10691, Stockholm, Sweden.
[c] Prof. Q. Zhao
Key Laboratory of Material Chemistry for Energy Conversion and Storage (Ministry of Education), School of Chemistry and Chemical Engineering
Huazhong University of Science and Technology
Luoyu Road No. 1037, Wuhan 430074, China
‡Authors contributing equally to the work.

Supporting information for this article is given via a link at the end of the document.

10.1002/anie.202002679

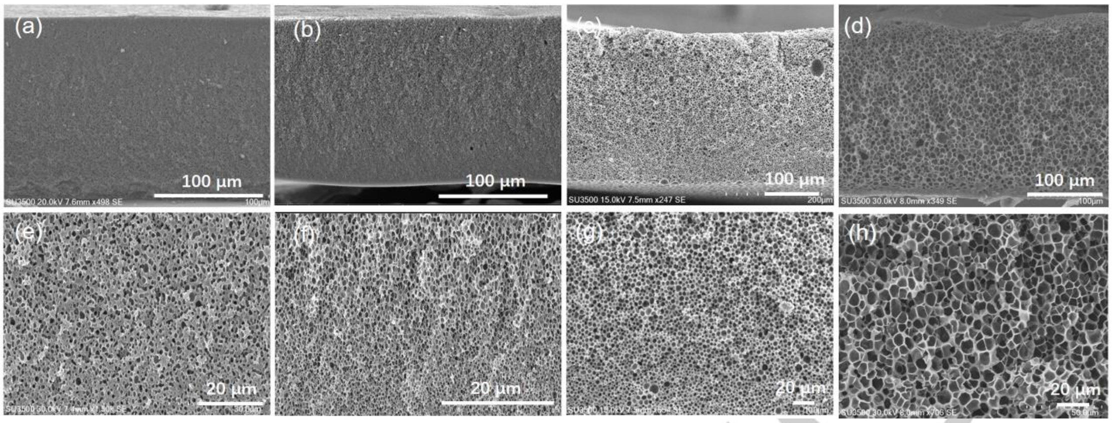

Figure 1. (a-d, and e-h) Low and high magnification cross-sectional SEM images of **SPPM-1**, **SPPM-2**, **SPPM-3** and **SPPM-4**, respectively, prepared from **PIL-1**, **PIL-2**, **PIL-3** and **PIL-4**, respectively, the PIL chemical structures are shown in Scheme 1.

Low-resolution cross-section scanning electron micrograph (SEM) images showed a three-dimensionally (3D) interconnected porous architecture for all four PILs tested here (Figure 1a-d). The average pore size for **SPPM-1** and **SPPM-4** was found to be 0.88±0.2 µm and 6.91±0.95 µm, respectively (Figure S15-16), while the micron pores in **SPPM-2** and **SPPM-3** are in a gradient distribution from top to bottom, which will be discussed later in detail.

To pinpoint the formation mechanism of SPPMs, a series of controlled experiments were conducted. The non-solvent-induced phase separation mechanism was first excluded because only a trace quantity of DMF solvent (<1 wt %) was left in the PIL film after 3 h of drying at 80 ºC. In elaborately designed control experiments using structurally similar polyvinylimidazlium counterparts of **PIL1-3** (Figure S17), that is, to replace the 1,2,4-triazolium cation in PIL by an imidazolium one, no freestanding SPPM formed. By contrast, **PIL-4**, which is also a polyvinylimidazolium but bears a carboxamide group could readily produce **SPPM-4**. Thus, both the heterocyclic cation and the alkyl substituent seem to impact the pore development. From a chemical structure viewpoint, the polarity of triazolium cations is known higher than that of imidazoliums owing to one additional nitrogen atom in the heterocyclic five-member ring; as for the substituent on the ring, the polarity of the amide group in **PIL-4** is higher than the methyl, cyanomethyl and 2-(ethylsulphanyl)ethyl ones in **PIL-1, 2** and **3**. In this regard, PILs with strong hydrogen bonding moiety was logically assumed to impact the SPPM formation. Molecular polarity was even strengthened by inclusion of water molecules in PIL matrices. Water molecules act as H-bonding cross-linker (*i.e.* donor and acceptor simultaneously) and promote a microphase separation of the hydrophilic cation ring in PILs from the hydrophobic framework consisting of the large-sized fluorinated counter anions (Tf_2N and Pf_2N), thereafter creating pores. The pore size of SPPMs increased by enhancing the polarity of the PIL cations and/or the hydrophobicity of the PIL anions (Figure S18), being consistent with SEM observations (Figure 1e-h).

As mentioned above, we noticed that the pore size in **SPPM-2** and **SPPM-3** gradually decreased from top to bottom sides. The pore size of **SPPM-2** decreases from the top layer 0.81±0.12 µm to bottom 0.33±0.06 µm, and for **SPPM-3**, from 4.51±0.73 to 2.42±0.70 µm, respectively. (Figure S19-20). These observations suggested that the formation of gradient porous structures was very plausibly determined by the diffusion of H_2O molecules into the PIL film from top to bottom. H_2O molecules became more difficult and slower to diffuse deeper into the film owing to a gradually weakened driving force for penetration. Such a gradient porous structure is promising in anti-reflection technology [18].

Interestingly, these SPPMs in the same time exhibited soft photoluminescence property (Figure S21). Therefore, the phase separation process of SPPMs could be monitored by laser scanning confocal microscopy (LSCM), as shown in Figure 2a-d. As observed, the pores developed rapidly in the first 12 hours, whereas only a slight expansion in pore size was noticed in the next 12 hours (Figure S22), which implies a spinodal-type mechanism[19].

In order to delve into how H_2O molecule coordinates via H-bonding with PIL in SPPMs, we conducted proton nuclear magnetic resonance (^1H-NMR) experiments for SPPM samples in different solvent environments. Taking **SPPM-1** for example, the blue line in Figure 2e displays its ^1H-NMR spectrum in DMSO-d_6. The C3 and C5 two proton signals in the 1,2,4-triazolium ring are clearly observed at 9.2 and 10.0 ppm, respectively. Interestingly, the C5 proton signal at 10.0 ppm high-lighted by an asterisk disappeared in a D_2O/DMSO-d_6 mixture (v/v=1:4) solvent, due to the well-known H/D exchange process. This result indicated that the C5-proton is highly active, and interacts with H_2O, which is further supported by the same ^1H-NMR experimental results of **SPPM-2** and **SPPM-3** (Figure S23-24). For **SPPM-4**, it was found that both C2-proton in imidazole ring and -NH_2 group can interact with water molecule (Figure S25).

Additional information that sheds light on H-bonding interactions of water with SPPMs was obtained from temperature-variable Fourier transfer inferred (FTIR) spectra (Figure 2f). The adsorption band centered at ~3400 cm^{-1} corresponds to the symmetric and antisymmetric stretching of water molecules in freeze-dried SPPM, and its intensity decreased with increasing temperatures, indicating a distinct coordination pattern of two hydroxyl groups with neighboring species of PILs.

Density functional theory (DFT) calculations revealed that water molecules are squeezed into domains between the triazolium ring and the polar -SO_2- moiety in Tf_2N anion. The introduced water

10.1002/anie.202002679

molecules, on the one side, weaken the Coulombic interactions between oppositely charged ions, whereas on the other side act as linkers connecting the triazolium ring and the -SO_2- moieties in the Tf_2N anion via two H-bonds (Figure S26-S29). An increase in temperatures leads to a gradual diminish of this water-featured adsorption band due to thermally weakened H-bonding interactions of water with triazolium rings and anions. Water molecules aggregate in polar domains in SPPMs forming small water clusters and large water pools, as verified from a clear visualization of distributions of water molecules in the **SPPM-1** matrix (Figure 2g). In addition, atomistic simulations showed that polar and apolar domains form gyroid interpenetrating phases in **SPPM-1** (Figure 2h), which promote a fast diffusion and distributions of water molecules in polar domains to bind the cation ring and the -SO_2- moieties in anions (Figure 2i) (Figure S30-33).

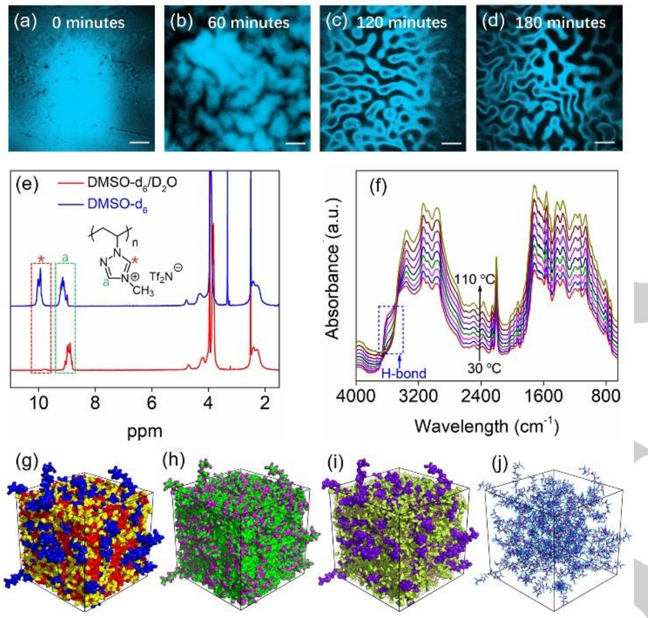

Figure 2. (a-d) Representative fluorescence LSCM 2D images of **SPPM-1** illuminated at 405 nm after soaking in water. Scale bar: 200 µm. (e) 1H NMR spectrum change of **SPPM-1** sample in different solvents (Testing condition: 10 mg of **SPPM-1** sample in 0.5 mL DMSO-d_6 vs 10 mg of **SPPM-1** sample in a mixture solvent of 0.1 mL of D_2O and 0.4 mL of DMSO-d_6). (f) In situ FTIR spectrum of the freeze-dried **SPPM-1**. (g-j) Representative liquid morphologies in **SMMP-1** containing water molecules (15% in mass ratio). (g) the PIL cation mainchain in blue, Tf_2N anion in yellow and water in red. (h) Polar domains in green and apolar domains in magenta. (i) PIL polar domains in purple, Tf_2N polar domains in yellow, and explicit water model in ball-stick model. (j) PIL framework with carbon atoms in mainchain (purple) and in pendant groups (cyan) and nitro-gen atoms (blue) in triazolium rings.

Integrating experimental and computational results, the formation mechanism of freestanding SPPMs can be attributed to H-bonding induced phase separation in SPPMs. Specifically, the introduction of water molecules into PIL network aggregates the PIL cations via preferential H-bonding interactions between polar domains, *i.e.* triazolium rings and water molecules. To be noted, the hydrophobic anions are obviously excluded from polar domains, leading to a strong phase separation of polar and apolar domains in PIL chains, and thereby constructing porous architectures. This model was further supported by the fact that poly((dimethyl-diallylammonium) bis(trifluoromethanesulfonyl)imide) (PDDA-Tf_2N) without active H species cannot develop porous membranes (Figure S34) because the tetraalkylammonium cation in PDDA cannot coordinate water molecules through H-bonding. Fair to say, the H-bond network is a necessity to form the pores.

It is noteworthy that such phase separation induced formation of porous membranes from a single homo-PIL was hard to achieve by traditional homopolymers. Although self-assembly of amphiphilic block copolymers could lead to porous films [20-23], the preparation process not only requires multiple tedious steps, *i.e.* rinsing with selective solvent and removal of additives and/or template, but also needs subtle design of the segments of block copolymers to modulate the mechanical stability of the film. In stark contrast, our membrane fabrication strategy is straightforward and scalable, suggesting that the process is more relevant to practical production.

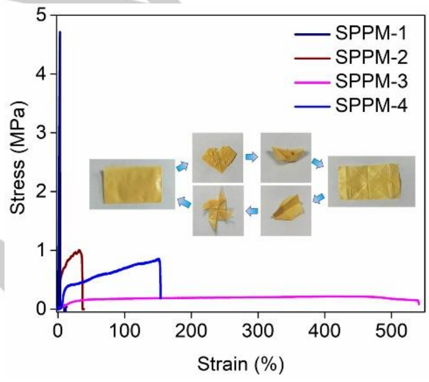

Figure 3. Tensile stress-strain curves of SPPMs. Inset is the photos of SPPM-2 that are folded with different shapes.

The mechanical property of membranes is crucial for their real-life usages. The stress-strain plot of SPPMs was recorded by tensile tests at a stretching speed of 50 mm min^{-1} under ambient conditions (40% relative humidity, 25 °C). As shown in Figure 3, **SPPM-1** exhibited a typical characteristic of brittleness with the maximum tensile stress up to 4.8 MPa and elongation of 3.2%. In stark contrast, **SPPM-3** displayed a remarkable elongation of 539% with an ultimate tensile stress up to 0.14 MPa, a typical characteristic of good ductileness. **SPPM-2** and **SPPM-4** showed elongation of 35% and 157% with ultimate tensile stress up to 1.0 MPa and 0.8 MPa, respectively, demon-strain their moderate toughness, which can be further testified by folding of **SPPM-2** into “heart”, “boat”, “windmill” or “plane” shapes in multiple times without damaging the membrane microstructure (inset of Figure 3). Essentially, the mechanical properties of SPPMs are tunable and closely relevant to the glass transition temperature of the corresponding PILs, as well as polarity (Figure S14). These results are intriguing as the mechanical properties of SPPMs ranging from brittleness to ductileness can be simply tailored by the rational choice of PIL structures.

Materials that dynamically and reversibly adapt transparency to environmental changes are widely studied because of both fundamental research interest and real-life applications in optical devices and security[24]. However, producing such devices is not easy due to the complicated strategies and limited choices of materials[25-26]. Typical temperature-dependent optical modulation devices were achieved through the control of liquid flow in porous substrates. [25] Noted that this process is hard to fine-tune their optical properties because of the unmanageable surface structure and chemistry of porous substrates. Meanwhile, materials such as poly(N-isopropylacrylamide) [27] with lower critical solution temperatures always display strong temperature dependent optical property in solution or gel, which is lost in a dried solid state. Hence, the development of membrane-like multifunctional materials that can be easily integrated into device components to modulate their transparency by variation of temperature is highly desirable.

In this context, we investigated the optical behaviour of the SPPMs upon thermal stimulus and water soaking. It was found that all SPPMs exhibited switchable optical properties towards temperature change (Figure S35-S37). Particularly, **SPPM-3** with a thickness of 250 μm could rapidly become pellucid from opaque within 5 minutes at 75 ºC (Figure S38), and the transmittance reached as high as 91% at a wavelength of 700 nm (Figure 4a). The optical switch triggered by thermal stimuli and water soaking process was highly reversible, and could be repeated over 20 cycles without noticeable change of optical transparency (Figure 4b).

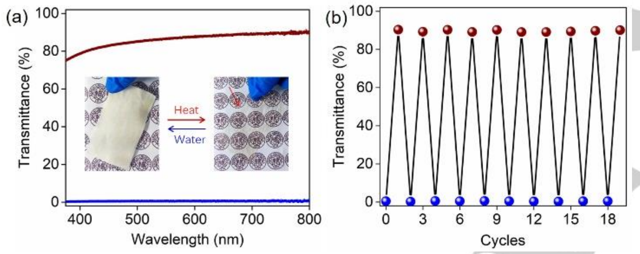

Figure 4. (a) UV-vis transmittance spectra of the porous (blue) and transparent state (purple) of **SPPM-3**, and their photographs. (b) Reversible optical switching of the **SPPM-3** at 700 nm over 20 cycles of heating and water soaking process.

The SEM images provided evidences of microstructural evolution of **SPPM-3** after switching back and forth of the optical transparency upon alternating thermal stimuli and water soaking processes. The pores of **SPPM-3** as expected vanished at elevated temperatures (Figure S39). It is understandable that enhanced temperatures dissociated the H-bond network of SPPMs; without the crosslinks by H-bonding, the pores closed due to a higher surface energy than a flat state, thereby turning the opal **SPPM-3** into a transparent nonporous thin film. To be noted that such a simple reversible porosion phenomenon is scarce [28], and this type of materials is of interest for separation, catalysis, optoelectronics, etc. In literatures, reported materials with reversible porosity behaviors are limited to systems based on photo- and chemical solvents stimulated azobenzene [29], and organic cage molecule [30]. Fair to say that our study offers an inspirating alternative to design and develop supramolecular porous polyelectrolyte membranes.

In summary, we demonstrated a facile and versatile one-pot approach toward scalable preparation of SPPMs by employing a single PIL crosslinked by H_2O molecules via hydrogen bonds. These SPPMs exhibit unique optical modulation ability accompanied by switchable porosity. We envision that by a judicious choice of PIL chemical structures, this straightforward fabrication strategy is capable of rational design of tunable, multifunctional adaptive materials for a diverse variety of applications.

Acknowledgements

H. W. acknowledges the financial support from the Nankai University, National Science Foundation of China (No. 21875119) and Natural Science Foundation of Tianjin (19JCYBJC17500). J.Y. thanks for a starting grant from the European Research Council with grant no. 639720-NAPOLI. We greatly appreciate Prof. Junqi Sun for fruit discussion.

Keywords: Supramolecular membrane • Poly(ionic liquid) • Reversible porosity • Noncovalent interaction

[1] J, Yu, N. E. Jackson, X. Xu, Y. Morgenstern, Y. Kaufman, M. Ruths, J. J. Pablo, M. Tirrell, *Science* **2018**, *360*, 1434-1438.
[2] K. Tybrandt, I. V. Zozoulenko, M. Berggren, *Sci. Adv.* **2017**, *3*, eaao3659.
[3] M. G. Cowan, D. L. Gin, R. D. Noble, *Acc. Chem. Res.* **2016**, *49*, 724.
[4] N. Alegret, A. Dominguez-Alfaro, D. Mecerreyes, *Biomacromolecules* **2019**, *20*, 73-89.
[5] M. Forsyth, L. Porcarelli, X. Wang, N. Goujon, D. Mecerreyes, *Acc. Chem. Res.* **2019**, *52*, 686-694.
[6] J. Y. Shin, S. A. Yamada, M. D. Fayer, *J. Am. Chem. Soc.* **2017**, *139*, 11222−11232.
[7] K. V. Peinemann, V. Abetz, P. F. W. Simon, *Nat. Mater.* **2007**, *6*, 992.
[8] G. Decher, *Science* **1997**, *227*, 1232-1237.
[9] W. Qian, J. Texter, F. Yan, *Chem. Soc. Rev.* **2017**, *46*, 1124-1159.
[10] J. Bartels, G. E. Sanoja, C. M. Evans, R. A. Segalman, M. E. Helgeson, *Macromolecules* **2017**, *50*, 8979-8987.
[11] Q. Zhao, M. Yin, A. P. Zhang, S. Prescher, M. Antonietti, J. Yuan, *J. Am. Chem. Soc.* **2013**, 135, 5549-5552.
[12] K. Zhang, X. Feng, X. Sui, M. A. Hempenius, G. J. Vancso, *Angew. Chem. Int. Ed.* **2014**, *53*, 13789.
[13] Y. Shao, Z. Jiang, Y. Zhang, T. Wang, P. Zhao, Z. Zhang, J. Yuan, H. Wang, *ACS Nano*, **2018**, 12, 11704-1710.
[14] T. Wang, Q. Wang, Y. Wang, Y. Da, W. Zhou, Y. Shao, D. Li, S. Zhan, J. Yuan, H. Wang, *Angew. Chem. Int. Ed.*, **2019**, *58*, 13600-13605.
[15] B. D. Amabilino, D. B. Smith, W. J. Steed, *Chem. Soc. Rev.*, **2017**, *46*, 2404-2420.
[16] E. Krieg, M. C. M. Bastings, P. Besenius, B. Rybtchinski, *Chem. Rev.* **2016**, 4, 2414-2477.
[17] R. J. Wojtecki, M. A. Meador, S. J. Rowan, *Nat. Mater.* **2011**, *10*, 14-27.
[18] J. Hiller, J. D. Mendelsohn, M. F. Rubner, *Nat. Mater.* **2002**, *1*, 59–63.
[19] T. C. Wang, B. Chen, M. F. Rubner, R. E. Cohen, *Langmuir* **2001**, *17*, 6610–6615.
[20] H. Hu, M. Gopinadhan, C. O. Osuji, *Soft Matter* **2014**, *10*, 3867-89.
[21] S. Ludwigs, A. Boker, A. Voronov, N. Rehse, R. Magerle, G. Krausch, *Nat. Mater.* **2003**, *2*, 744-747.
[22] A. Sidorenko, I. Tokarev, S. Minko, M. Stamm, *J. Am. Chem. Soc.* **2003**, *125*, 12211-12216.
[23] H. Sai, K. W. Tan, K. Hur, E. Asenath-Smith, R. Hovden, Y. Jiang, M. Riccio, D. A. Muller, V. Elser, L. A. Estroff, S. M. Gruner, U. Wiesner, *Science* **2013**, *341*, 530-534.
[24] D. Ge, E. Lee, L. Yang, Y. Cho, M. Li, D. S. Gianola, S. A. Yang, *Adv. Mater.* **2015**, *27*, 2489–2495.

[25] K. Manabe, T. Matsubayashi, M. Tenjimbayashi, T. Moriya, Y. Tsuge, K. H. Kyung, S. Shiratori, *ACS Nano* **2016**, *10*, 9387−9396.

[26] C. H. Lee, H. S. Lim, J. Kim, J. H. Cho, *ACS Nano* **2011**, *5*, 7397–7403.

[27] T. M. Fulghum, N. C. Estillore, C. D. Vo, S. P. Armes, R. C. Advincula, *Macromolecules* **2008**, *41*, 429−435.

[28] Y. Feng, T. John, *Angew. Chem. Int. Ed.* **2007**, *46*, 2440-2443.

[29] M. Baroncini, S. Agostino, G. Bergamini, P. Ceroni, A. Comotti, P. Sozzani, I. Bassanetti, F. Grepioni, T. M. Hernandez, S. Silvi, M. Venturi, A. Credi, *Nat. Chem.* **2015**, *7*, 634-640.

[30] J. T. A. Jones, D. Holden, T. Mitra, T. Hasell, D. J. Adams, K. E. Jelfs, A. Trewin, D. J. Willock, G. M. Day, J. Bacsa, A. Steiner, A. I. Cooper, *Angew. Chem. Int. Ed.* **2011**, *50*, 749 –753

COMMUNICATION

Supramolecular porous polyelectrolyte membranes is constructed by utilizing water as cross-linker from a single poly(ionic liquid). Owing the intrinsic dynamic nature of hydrogen bonding, these SPPMs could switch porosity upon thermal stimuli, which is exemplified by dynamically adaptive transparency to thermal fluctuation.

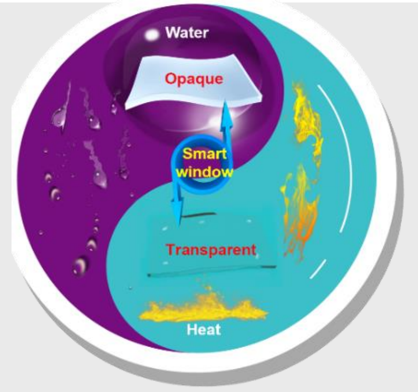

Yue Shao[a‡], Yong-Lei Wang[b‡], Xiangshuai Li[a], Atefeh Khorsand Kheirabad[b], Qiang Zhao[c], Jiayin Yuan[b], Hong Wang[a]*

Page No. – Page No.

Water can Crosslink a Single Poly(ionic liquid) into Porous Supramolecular Membranes